



Advances on Soil-Structure Interaction Analysis through the Simulation of Forced Vibration Tests for a Building Model on the Actual Ground

T. Abiru⁽¹⁾, M. Akiyama⁽²⁾, E. Ochiai⁽³⁾, H. Sugita⁽⁴⁾, T. Nozawa⁽⁵⁾, Y. Mihara⁽⁶⁾

⁽¹⁾ Manager, Chugoku Electric Power Co., Inc., Japan, 368753@pnet.energia.co.jp

⁽²⁾ Assistant Manager, Chugoku Electric Power Co., Inc., Japan, 264707@pnet.energia.co.jp

⁽³⁾ Staff Assistant Manager, Chugoku Electric Power Co., Inc., Japan, 277789@pnet.energia.co.jp

⁽⁴⁾ General Manager, Kajima Corporation, Japan, sugita-hiro@kajima.com

⁽⁵⁾ Senior Manager, Kajima Corporation, Japan, nozawat@kajima.com

⁽⁶⁾ Deputy Senior Manager, Kajima Corporation, Japan, y-mihara@kajima.com

Abstract

We presented about the forced vibration tests for a large-scale reinforced concrete building model constructed on the actual site ground with various backfill conditions and confirmed the applicability of conventional design method for linear soil-structure interaction behavior with the embedment effects in case of limited range of soil improvement^[1]. Based on the previous study, this study focuses on more detail analyses of a number of vibration tests using large exciter in which nonlinear soil-structure interaction behavior was observed. The brief overview of this paper is as indicated below.

First, microtremor observation analyses before and after a number of forced vibration tests using large exciter show that nonlinear soil-structure interaction behavior is caused by not plastic phenomena of soil or building itself but the change of boundary condition between soil and building.

Second, more detail analyses of a number of forced vibration tests using large exciter are performed from the viewpoints of harmonic components and chronological change of response records of the soil surrounding the building. Their results show the geometrical nonlinear effect such as contact, slip and separation phenomena between side soil and building in a qualitative manner.

Finally, to understand nonlinear soil-structure interaction behavior in more detail, numerical simulation analyses of soil-structure interaction (SSI) are performed comparing to the test results. To take into account for contact, slip and separation phenomena which were observed between surrounding soil and building based on the above test results, the joint elements are introduced in the soil-structure interface. Using 3-dimensional finite element method (3-D FEM) for SSI with joint parameters such as friction coefficient between soil and building, simulation analyses for the a number of vibration tests using not only small but also large exciters are achieved to confirm the applicability of more suitable model for evaluating the embedment effects.

Keywords: Forced Vibration Test, Nonlinear Soil-Structure Interaction, 3-D FEM, Embedment Effect, Geometrical Nonlinear Effect



1. Introduction

We presented about the forced vibration tests for a large-scale reinforced concrete building model constructed on the actual site ground with various backfill conditions and confirmed the applicability of conventional design method for linear soil-structure interaction behavior with the embedment effects in case of limited range of soil improvement [1]. The vibration tests include several forced vibration tests using large exciter in which nonlinear soil-structure interaction behavior was observed and also microtremor observations before and after several forced vibration tests.

Based on more detail analyses of the above vibration test results, the objective of this study is to enhance the advancement on nonlinear soil-structure interaction model through the numerical simulation analysis of forced vibration tests using large exciter.

2. Outline of Vibration Tests

The program of vibration tests including several forced vibration tests and microtremor observations is shown in Table 1. Location of exciter and sensors including geometry of the soil and building model is shown in Fig.1. Large exciter for maximum excitation force 98kN is located at the roof of the building model and in forced vibration tests, sinusoidal excitation forces such as 19.6kN, 49.0kN and 98.0kN are applied in x direction at 2 to 20Hz frequency. Excitation forces are applied from low frequency to high frequency except L-10(3). Velocimeters are used for measurement. After exciter becomes stable at a prescribed frequency, velocity time history of total 100 waves is recorded at at least 180-point sampling frequencies per one wave.

Resonance and phase lag curves corresponding to horizontal displacement on the roof are shown in Fig.2. Peak frequency becomes lower from 14.0Hz to 11.0Hz if excitation force increases. L-10(2) and L-10(3) are almost the same and L-10(1) is also similar to them only for higher than the peak frequency. Comparing to the above 3 large excitation cases, it is implicated that dynamic characteristics drastically changes around the peak frequency in first large excitation case L-10(1).

Table 1 – Program of vibration tests

Test date	Forced vibration test			Microtremor observation
	Excitation force 98.0kN	Excitation force 49.0kN	Excitation force 19.6kN	
Day 1~3				[~L-2(1)]
Day 4		L-5	L-2(1)	[L-5~L-10(1)]
Day 5	L-10(1)			[L-10(1)~L-10(2)]
Day 6	L-10(2)			[L-10(2) ~L-2(2)]
Day 7			L-2(2)	[L-2(2)~L-10(3)]
Day 8				
Day 9	L-10(3)			[L-10(3)~]
Day 10, 11				

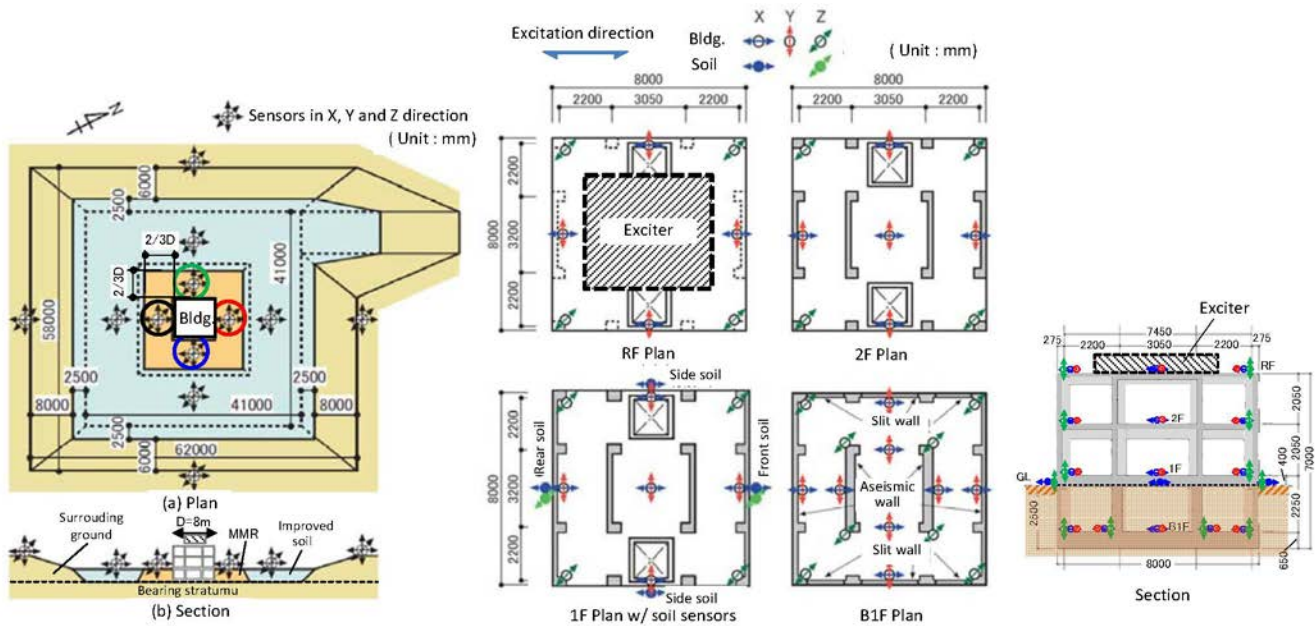


Fig. 1 – Location of exciter and sensors

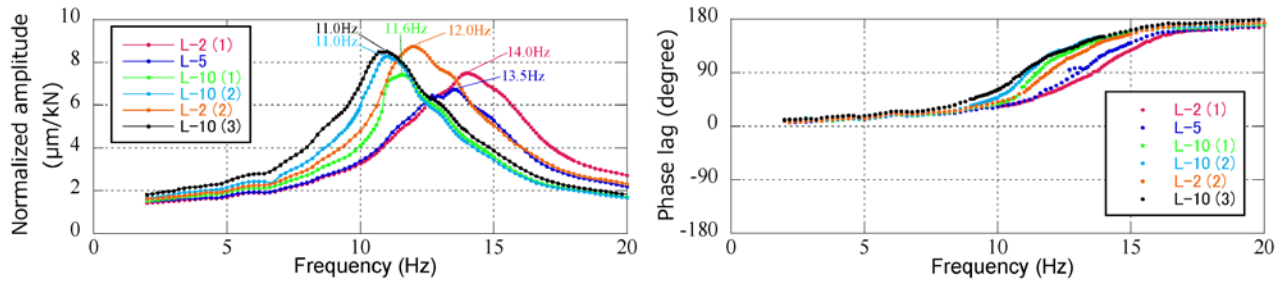


Fig. 2 – Resonance and phase lag curves corresponding to horizontal displacement on the roof

3. Microtremor Observation

Microtremor observations before and after several forced vibration tests are successively conducted for 163.84sec per frame and 200Hz sampling as shown in Table 1. However, since aftershock of the 2011 off the Pacific coast of Tohoku earthquake occurred frequently during the test, observation records include a lot of very far and small earthquakes. Therefore, ensemble average treatment is processed by eliminating the abnormal frames caused by earthquakes.

Transfer function in the building RF to B1F is shown in Fig. 3. Dynamic characteristics of the building itself such as peak frequency, shape, amplitude and phase seems to be the same before and after forced vibration tests while randomness near the peak of 14 to 15Hz is slightly observed because of minim input denominator at microtremor measurement.

To confirm the change of dynamic characteristics of the surrounding soil before and after forced vibration tests, spectrum ratio of horizontal to vertical components (H/V ratio) is shown in Fig. 4. In the figure, H/V ratio in x direction is written in solid line and also that in y direction is written in dotted line for the sensors' location noted in circle shown in Fig. 1. The trend of both figures is extremely similar and thus it is confirmed that dynamic characteristics of the surrounding soil does not change before and after forced vibration tests. For reference, the peak around 4 to 5 Hz is supposed to be corresponding to material properties of the backfilled soil.

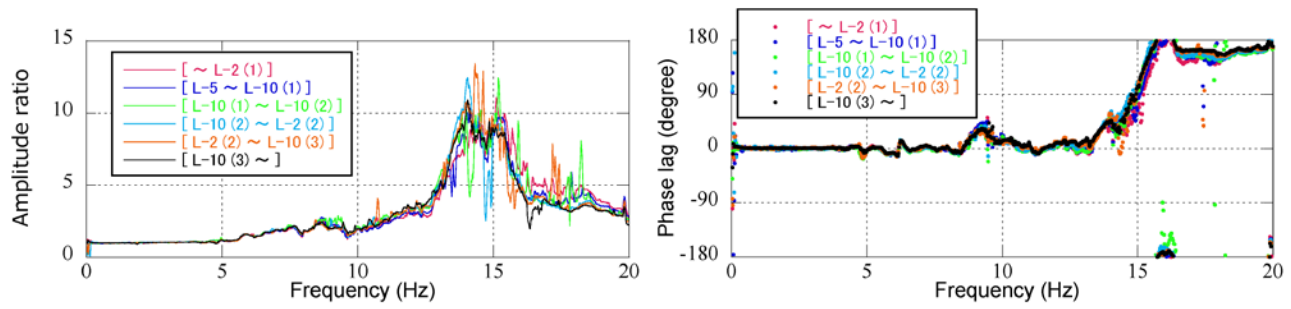


Fig. 3 – Transfer function in the building RF to B1F

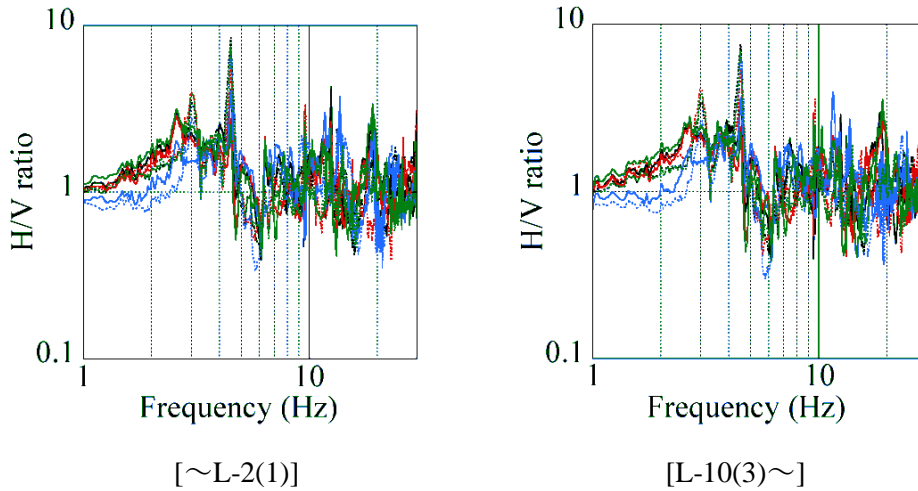


Fig. 4 – Comparison of H/V ratio

4. Forced Vibration Test Using Large Exciter

4.1 Analysis by harmonic components

Excitation force in forced vibration test contains harmonic components even in the case of applied sinusoidal excitation at a specific frequency. Since 3rd harmonic component is presented to be stable in this test, comparison between 1st and 3rd harmonic components regarding phase lag of displacement at the roof is shown in Fig. 5 by adjusting frequency range except L-10(3). For small excitation forces such as L-2(1), L-2(2) and L-5, phase lags evaluated from 1st and 3rd harmonic components are corresponding well up to 20Hz and thus they are supposed to behave linearly. On the other hand, for large excitation forces such as L-10(1) and L-10(2), phase lags evaluated from 1st and 3rd harmonic components have some gaps around 10 to 14Hz. Therefore, they are supposed to behave non-linearly at such frequency ranges. Moreover, comparing between L-2(1) and L-2(2), the latter is shifting to slightly lower frequency level. That is assumed because L-2(2) has a large excitation experience.

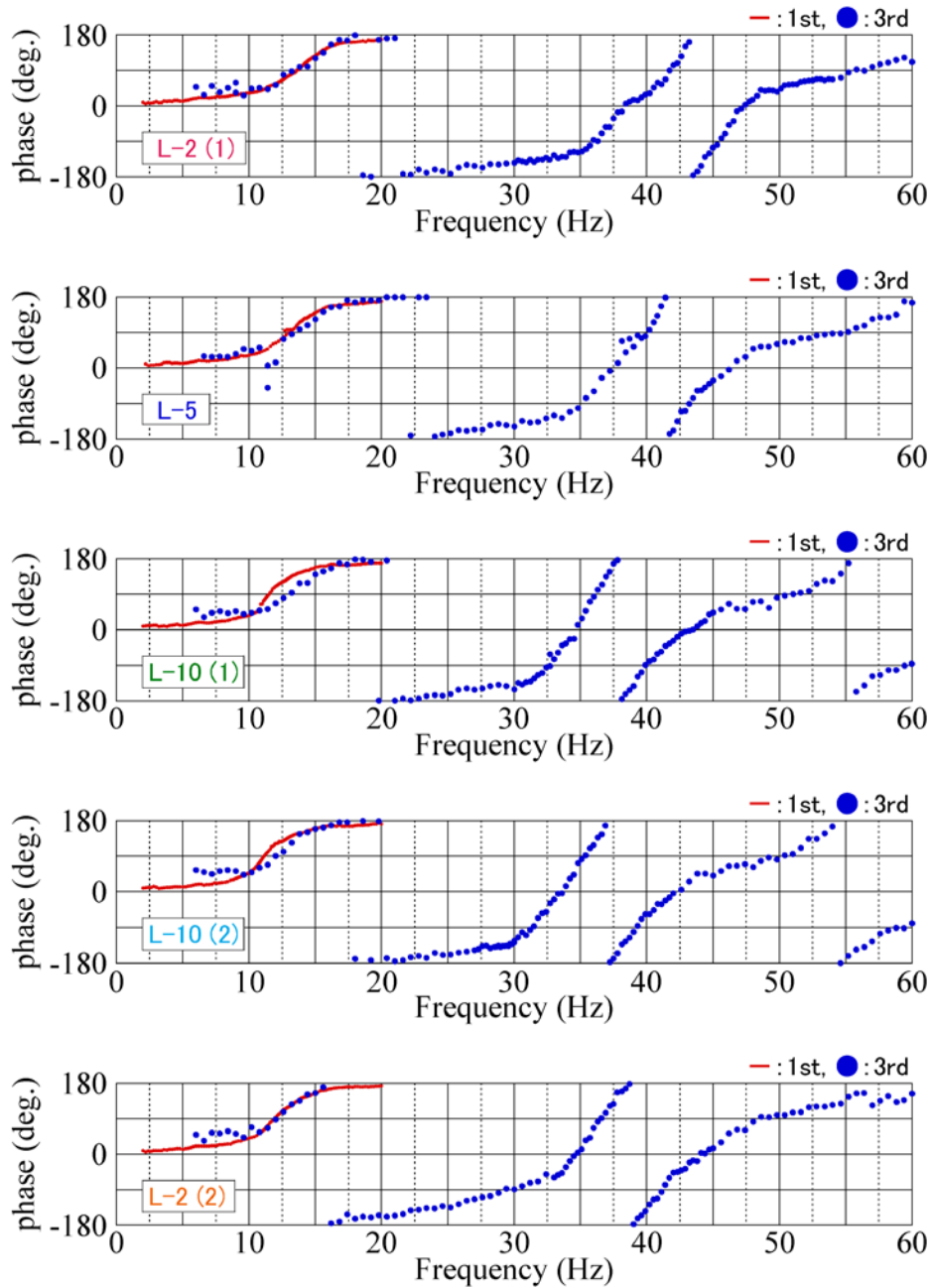


Fig. 5 – Comparison between 1st and 3rd harmonic components regarding phase lag at the roof

4.2 Analysis by response records of soil adjacent to building

For the front soil adjacent to building in the direction of applied force, velocity time history and Fourier spectrum at typical frequencies in L-10(1) are shown in Fig. 6. For 3.0Hz excitation, harmonic components are small. On the other hand, for 11.6Hz excitation of peak frequency, wave distortion is larger and 2nd and 3rd harmonic components are relatively large.

For 11.0Hz excitation of peak frequency in L-10(2) and L-10(3), velocity time histories after L-10(1) of the front and rear soil adjacent to building in the direction of applied force are shown in Fig. 7. The followings are observed:

- The front and rear soil show opposite phases at wave distortion parts.

- While L-10(2) and L-10(3) are quite similar, wave distortion in L-10(1) is relatively small. Thus, L-10(1) is supposed to be transitional state up to strong nonlinearity.
- Slight wave distortion even in small excitation L-2(2) is observed because of nonlinear effect by large excitation experience.

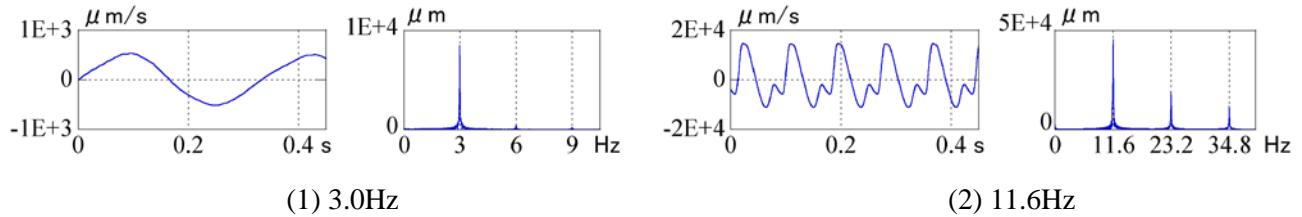


Fig. 6 – Velocity time history and Fourier spectrum at typical frequencies in L-10(1)

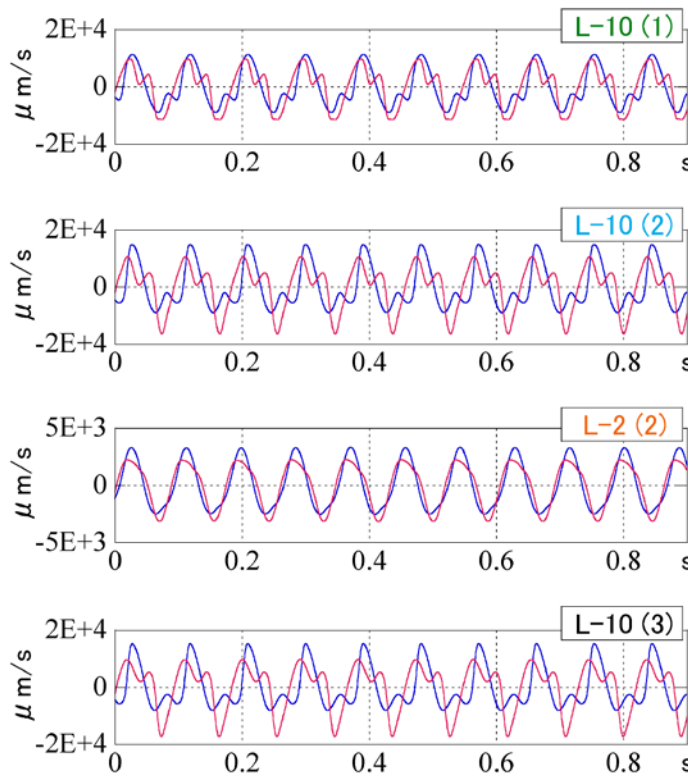


Fig. 7 – Velocity time histories after L-10(1) [—: front, - -: rear ; 11.0Hz]

4.3 Analysis by response records between side soil and building

Displacements of side soil and building at ground level are compared. Displacement of the building are linearly interpolated using that of 1F and B1F. Displacement ratio of soil to building is calculated in Fig. 8 except for the effects of displacement at B1F. The followings are observed:

- For L-2(1), building is almost in contact with side soil because displacement ratio is close to 1.
- For L-5, building is almost in contact with side soil up to around 12Hz but it is slightly separated from side soil at higher frequency than 12Hz.
- For L-10(1), slight separation between building and side soil seems to occur up to around 10Hz similar to L-5. At higher frequency than 10Hz, large separation seems to occur because displacement ratio significantly decreases.

- For L-10(2), L-2(2) and L-10(3), large separation between building and side soil seems to occur similar to that at higher frequency than 10Hz in L-10(1).
- Chronological change of amplitude ratio also shows large separation between building and side soil after L-10(1).

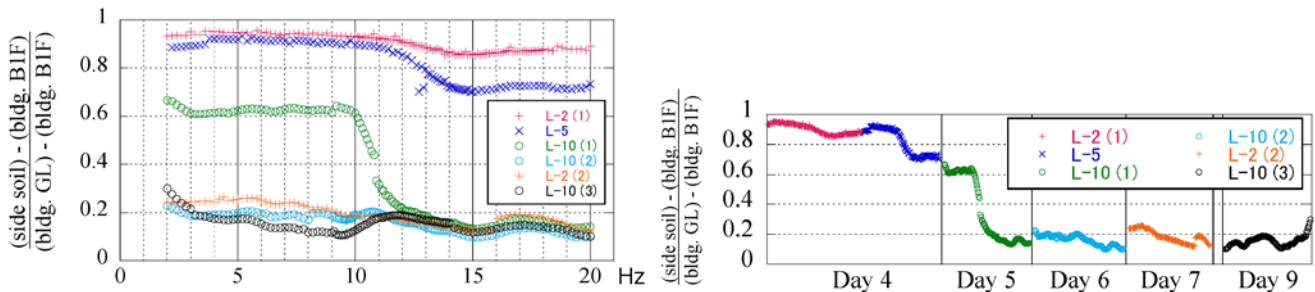


Fig. 8 – Displacement ratio of soil to building

5. Numerical Simulation Analyses using 3-D FEM Model

5.1 Analytical condition

5.1.1 Simulation target

To focus on the geometrical nonlinear effect such as contact, slip and separation phenomena between surrounding soil and building described in chapter 4, simulation targets are small excitation case (C3-RX) ^[1] which does not show the geometrical nonlinear effect and also two large excitation cases (L-10(1) and L-10(2)) which show different geometrical nonlinear effects.

5.1.2 FEM model

Numerical simulation analyses are performed by applying sinusoidal excitation force on the roof using 3D-FEM model for soil and building. As referred to previous small excitation simulation analyses ^[1], soil is modeled in 50m x 50m dimension and 15m depth. Soil and building is also modeled as half symmetry to x direction.

Soil and building foundation are modeled as solid element. Wall and slab of the building are modeled as layered shell element. Column and beam of the building are modeled as beam element. The boundary of soil is modeled as infinite element which is expressed as semi-infinite boundary condition. To take into account for contact, slip and separation phenomena which were observed between surrounding soil and building based on the result in chapter 4, the joint elements are introduced in the soil-building interface.

Mesh size of building and adjacent soil is 0.5m to trace geometrical nonlinear effect between surrounding soil and building. Mesh size of soil deeper than bearing stratum #2 is 1.0m similar to previous small excitation simulation analyses ^[1]. Soil-building 3-D FEM model is shown in Fig. 9.

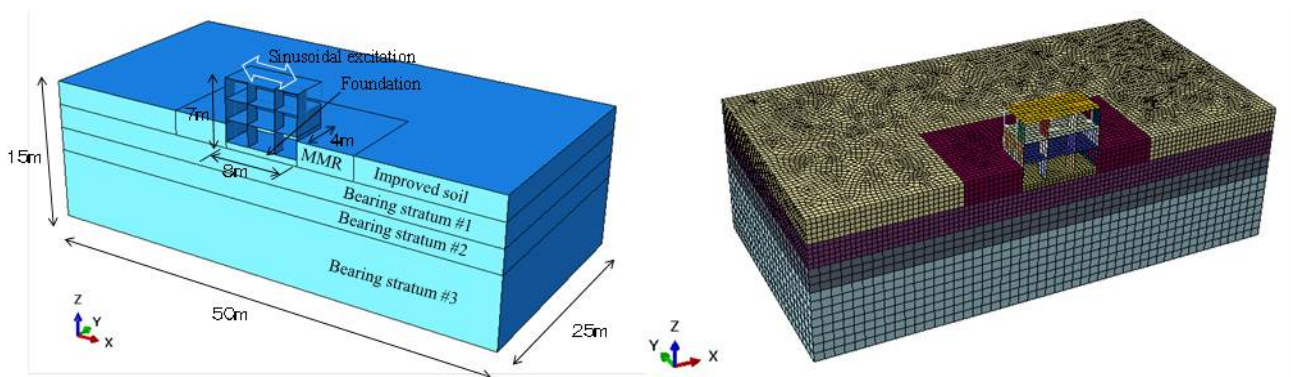


Fig. 9 – Soil-building 3-D FEM model



5.1.3 Material property

Based on the result in chapter 3, soil and building are assumed to be elastic in numerical simulation analyses. Material property of soil and building is similar to previous small excitation simulation analyses ^[1]. Material property of soil is shown in Table 2. Material properties of building are $E=34.2\text{kN/mm}^2$ for Young's modulus, $G=13.3\text{kN/mm}^2$ for shear modulus and 3% for damping factor. For slip between surrounding soil and building, adhesion is assumed to be ignored and coefficients of friction are varied as parametric study.

Table 2 – Material property of soil

Soil	Shear wave velocity	Poisson's ratio	Wet density	Damping factor
Bearing stratum #1	275m/s	0.37	1.80 g/cm ³	0.05
Bearing stratum #2	279m/s	0.38	1.80 g/cm ³	0.05
Bearing stratum #3	378m/s	0.37	1.80 g/cm ³	0.05
MMR	257m/s	0.32	1.87 g/cm ³	0.05
Improved soil	167m/s	0.36	1.87 g/cm ³	0.07

5.1.4 Loading condition

For loading condition, only one sinusoidal excitation force is dynamically applied in x direction at the location of exciter after gravity load is applied. Excitation frequency range is basically 8 to 14Hz which covers the peak frequency in the tests.

5.2 Analytical results

5.2.1 Simulation results

For small excitation case (C3-RX) and two large excitation cases (L-10(1) and L-10(2)), comparison of resonance curves corresponding to horizontal displacement on the roof with varied coefficients of friction as parameters are shown in Fig. 10.

As the results, numerical simulation analysis using 3D-FEM for small excitation case (C3-RX) corresponds well to the test result with firmly fixed boundary condition between surrounding soil and building similar to previous small excitation simulation analyses ^[1]. For large excitation case, numerical simulation analysis also corresponds well to the test result with geometrical nonlinear effect such as contact, slip and separation phenomena between surrounding soil and building. Especially, for 1st large excitation case (L-10(1)), numerical simulation analysis corresponds well to the test result with coefficient of friction 0.8. For 2nd large excitation case (L-10(2)), numerical simulation analysis corresponds well to the test result with smaller coefficient of friction 0.5 comparing to 1st large excitation case (L-10(1)).

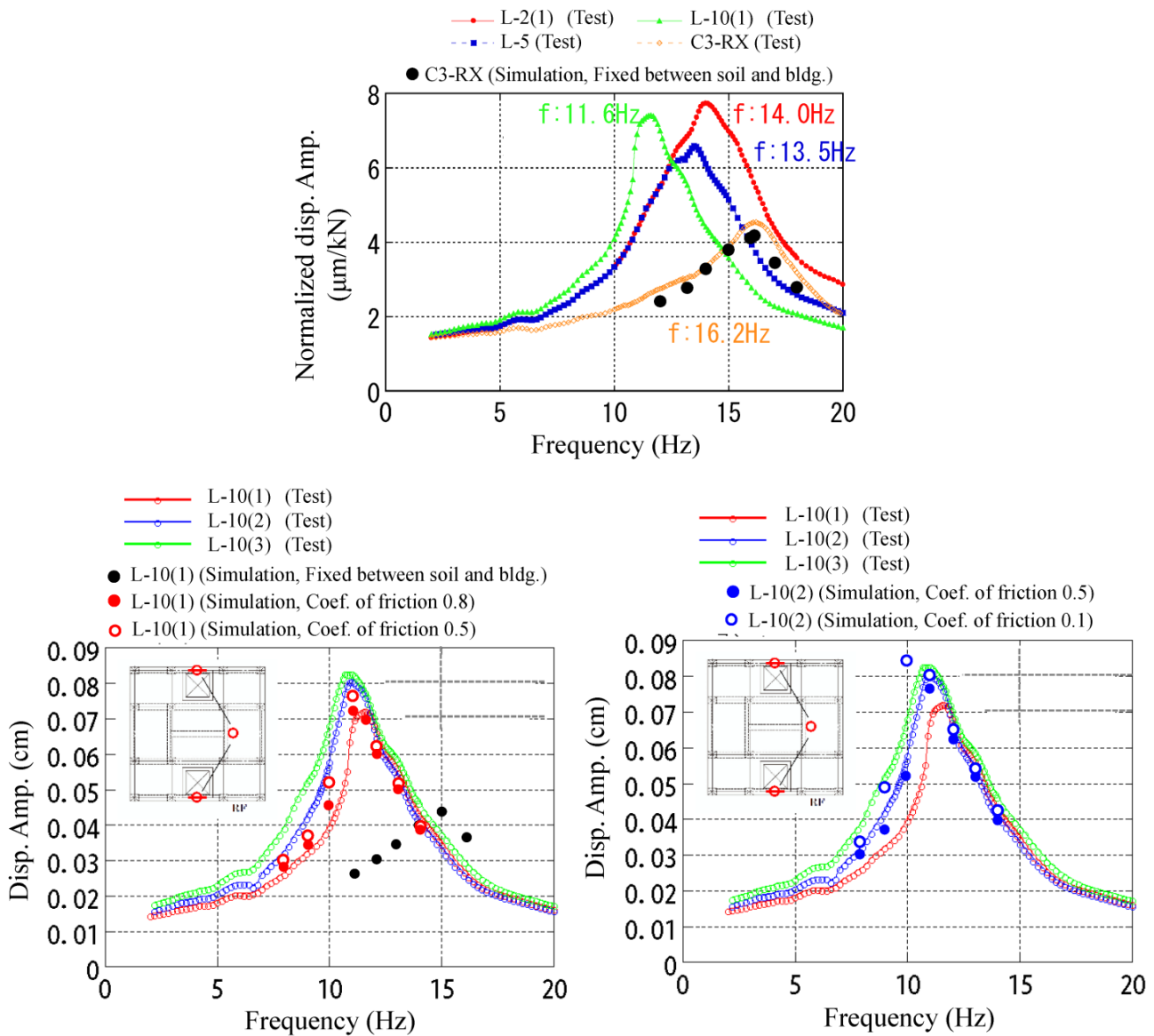


Fig. 10 – Comparison of resonance curves corresponding to horizontal displacement on the roof

5.2.2 Influence on number of large excitation

Influence on number of large excitation is numerically studied by applying two sinusoidal excitation forces for 1st large excitation case (L-10(1)) with coefficient of friction 0.8. For 11.6Hz excitation of peak frequency, comparison of velocity time histories of the front soil adjacent to building in the direction of applied force is shown in Fig. 11. As the results, there are no big differences between 1st and 2nd wave by numerical result and both waves by numerical result correspond well to the test result. Therefore, even for large excitation case in which nonlinear soil-structure interaction behavior was observed, numerical simulation analysis using only one sinusoidal excitation force corresponds enough well to the test result.

5.2.3 Strain level of surrounding soil

From numerical simulation analysis results for 1st large excitation case (L-10(1)) with coefficient of friction 0.8, minimum principal strain contour of surrounding soil is shown in Fig. 12 at the time of maximum displacement at the roof for peak frequency 11.6Hz. Since maximum compressive principal strain of soil is 0.02% to 0.03%, soil is enough within elastic range. That is corresponding to microtremor observation before and after forced

vibration tests shown in chapter 3. Moreover, maximum tensile principal strain of soil is an order of magnitude smaller than compressive one.

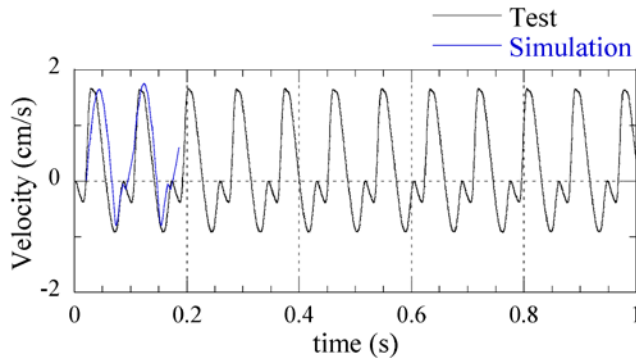


Fig. 11 – Comparison of velocity time histories

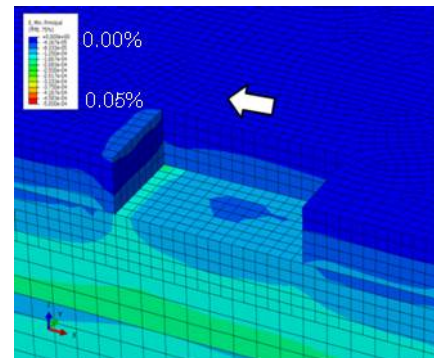


Fig. 12 – Minimum principal strain of soil

5.2.4 Contact pressure between soil and building

From numerical simulation analysis results for 1st large excitation case (L-10(1)) with coefficient of friction 0.8, contact pressure contour between surrounding soil and building is shown in Fig. 13 at the time of maximum displacement at the roof for peak frequency 11.6Hz. Since blue parts are corresponding to the separation area between surrounding soil and building, upper half of embedment soil is almost separated from building for the rear soil adjacent to building in the direction of applied force. Also, all areas of embedment soil are in fully contact with building for the front soil adjacent to building in the direction of applied force. Moreover, slightly deep areas of embedment soil from the ground are separated from building for the side soil adjacent to building in the direction of applied force.

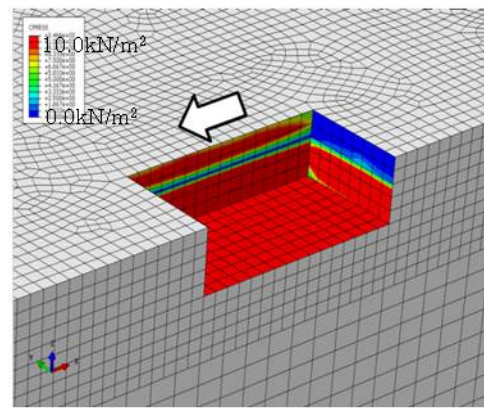
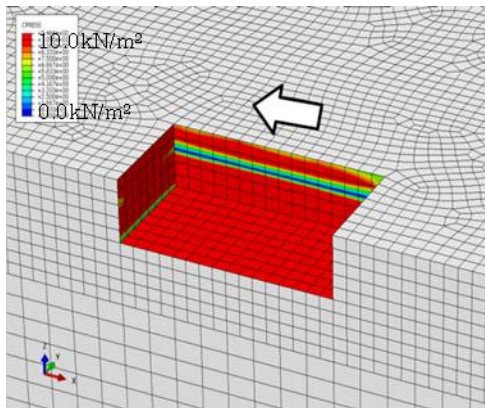


Fig. 13 – Contact pressure contour between surrounding soil and building

5.2.5 Shear stress by friction between soil and building

From numerical simulation analysis results for 1st large excitation case (L-10(1)) with coefficient of friction 0.8, shear stress contours by friction between surrounding soil and building are shown in Fig. 14 to Fig. 15 at the time of maximum displacement at the roof for peak frequency 11.6Hz. Due to not only confining pressure of soil but also out-of-plane deformation of basement wall itself, very complicated horizontal shear stress distribution is observed in a longitudinal direction for the side soil adjacent to building in the direction of applied force. Considering the area where shear stress is relatively small, almost half of embedment soil is sliding from building for the side soil adjacent to building in the direction of applied force. On the other hand, vertical shear stress distribution is almost uniform in depth for all trihedral side soils adjacent to building.

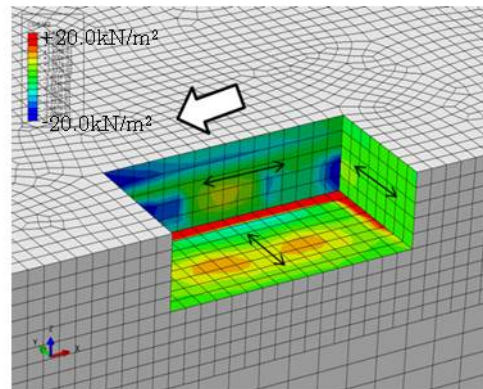
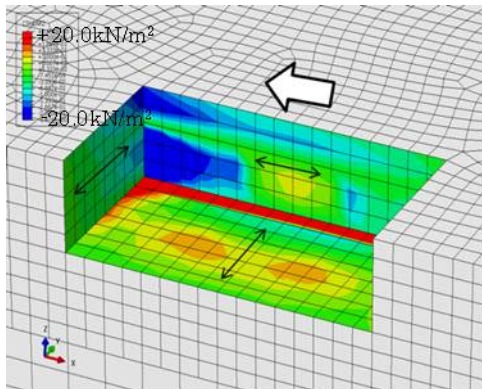


Fig. 14 – Horizontal shear stress caused by friction between surrounding soil and building

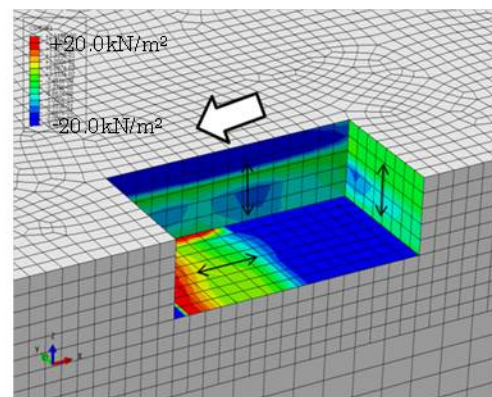
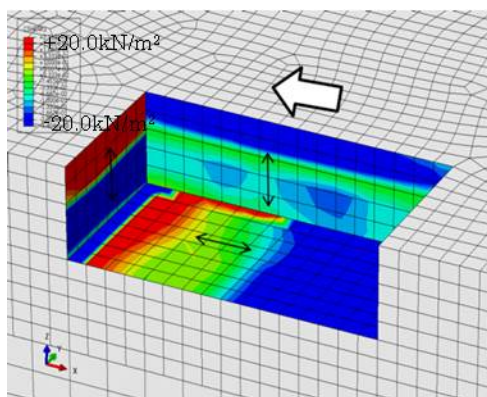


Fig. 15 – Vertical shear stress caused by friction between surrounding soil and building

6. Conclusion

Based on the previous study ^[1], this study focuses on more detail analyses of a number of vibration tests using large exciter in which nonlinear soil-structure interaction behavior was observed. The brief conclusion in each chapter is briefly summarized in the following.

6.1 Outline of vibration tests

- The vibration tests include several forced vibration tests using large exciter in which nonlinear soil-structure interaction behavior was observed and also microtremor observations before and after several forced vibration tests.
- Nonlinear soil-structure interaction behavior was observed such that peak frequency becomes lower as excitation force increases.

6.2 Microtremor observation

- Microtremor observation analyses before and after a number of forced vibration tests using large exciter show that nonlinear soil-structure interaction behavior is caused by not plastic phenomena of soil or building itself but the change of boundary condition between soil and building.

6.3 Forced vibration test using large exciter

- Since phase lags evaluated from 1st and 3rd harmonic components have some gaps, they are supposed to behave non-linearly at specific frequency range.
- Based on velocity time histories of the front and rear soil adjacent to building in the direction of applied force, wave distortion is larger and harmonic components are also relatively large according to nonlinear level.



- Based on chronological change of response records of the soil adjacent to the building, the geometrical nonlinear effect such as contact, slip and separation phenomena between side soil and building is characterized in a qualitative manner.

6.4 Numerical simulation analyses using 3-D FEM model

- Numerical simulation analysis using 3D-FEM corresponds well to the test result for not only small excitation case but also large excitation case with geometrical nonlinear effect such as contact, slip and separation phenomena between surrounding soil and building.
- For 1st large excitation case (L-10(1)), numerical simulation analysis corresponds well to the test result with coefficient of friction 0.8. For 2nd large excitation case (L-10(2)), numerical simulation analysis corresponds well to the test result with smaller coefficient of friction 0.5 comparing to 1st large excitation case (L-10(1)).
- Even for large excitation case in which nonlinear soil-structure interaction behavior was observed, numerical simulation analysis using only one sinusoidal excitation force corresponds enough well to the test result.
- As the results for 1st large excitation case, strain level of surrounding soil is enough within elastic range that is corresponding to microtremor observation before and after forced vibration tests.
- As the results for 1st large excitation case, upper half of embedment soil is almost separated from building for the rear soil adjacent to building in the direction of applied force. Also, all areas of embedment soil are in fully contact with building for the front soil adjacent to building in the direction of applied force.
- Regarding shear stress caused by friction between surrounding soil and building for 1st large excitation case, due to not only confining pressure of soil but also out-of-plane deformation of basement wall itself, very complicated horizontal shear stress distribution is observed in a longitudinal direction for the side soil adjacent to building in the direction of applied force. Considering the area where shear stress is relatively small, almost half of embedment soil is sliding from building for the side soil adjacent to building in the direction of applied force.

7. Acknowledgements

We would like to express our deep appreciation to Dr. Yuji Miyamoto, Professor of Osaka University, and Dr. Koichi Kusunoki, Associate Professor of the University of Tokyo, for their guidance throughout this research.

8. References

- [1] T. Abiru, T. Hashimoto, E. Ochiai, H. Sugita, Y. Suzuki, K. Iwamoto and H. Murakami (2012): Embedment Effects by Forced Vibration Tests and Analysis of a Large-scale Building Model on the Actual Ground. *15 WCEE*, Lisbon, Portugal.